Development 134, 2115-2124 (2007) doi:10.1242/dev.02850

Regulation of ventral midbrain patterning by Hedgehog signaling

Roy D. Bayly[1], Minhtran Ngo[2,*], Galina V. Aglyamova[2] and Seema Agarwala[1,2,3,†]

In the developing ventral midbrain, the signaling molecule sonic hedgehog (SHH) is sufficient to specify a striped pattern of cell fates (midbrain arcs). Here, we asked whether and precisely how hedgehog (HH) signaling might be necessary for ventral midbrain patterning. By blocking HH signaling by in ovo misexpression of *Ptc1*$^{\Delta loop2}$, we show that HH signaling is necessary and can act directly at a distance to specify midbrain cell fates. Ventral midbrain progenitors extinguish their dependence upon HH in a spatiotemporally complex manner, completing cell-fate specification at the periphery by Hamburger and Hamilton stage 13. Thus, patterning at the lateral periphery of the ventral midbrain is accomplished early, when the midbrain is small and the HH signal needs to travel relatively short distances (approximately 30 cell diameters). Interestingly, single-cell injections demonstrate that patterning in the midbrain occurs within the context of cortex-like radial columns of cells that can share HH blockade and are cytoplasmically connected by gap junctions. HH blockade results in increased cell scatter, disrupting the spatial coherence of the midbrain arc pattern. Finally, HH signaling is required for the integrity and the signaling properties of the boundaries of the midbrain (e.g. the midbrain-hindbrain boundary, the dorsoventral boundary), its perturbations resulting in abnormal cell mixing across 'leaky' borders.

KEY WORDS: Midbrain-hindbrain boundary, Motor and dopaminergic neurons, Morphogen, Cell affinities, Size regulation, Midbrain radial columns, Chick

INTRODUCTION

The developmental organization of any tissue requires the coordination of signals that emanate from specialized signaling centers located at tissue boundaries (Rubenstein et al., 1994). In the case of the midbrain, the identity of the ventral midbrain or rostral floor plate (rFP) as a signaling center is firmly established (Agarwala et al., 2001; Blaess et al., 2006; Fedtsova and Turner, 2001). The rFP occupies the ventral midline of the midbrain and secretes the signaling molecule sonic hedgehog (SHH), whose role in pattern formation is the focus of intense study (Ingham and McMahon, 2001).

Hedgehog (HH) signal transduction begins with HH binding to its receptor and negative regulator, PTC1 (Hooper and Scott, 2005; Ingham and McMahon, 2001; Marigo et al., 1996; Stone et al., 1996). In the absence of HH signaling, PTC1 maintains a constitutive block on the transmembrane protein smoothened (SMO) so that no signaling can occur (Akiyama et al., 1997; Alcedo et al., 1996). New findings suggest that, in the absence of the ligand, PTC1 can induce provitamin D3, which binds SMO in adjacent cells to block HH activation (Bijlsma et al., 2006). In the presence of HH, the PTC1-mediated block on SMO is lifted. HH signaling then occurs via a complex cascade, which eventually converges upon the activator- (GLI1, GLI2, GLI3) or repressor- (chiefly GLI3) function of the GLI/Ci family of transcription factors (Aza-Blanc et al., 1997; Bai et al., 2004; Dai et al., 1999; Litingtung and Chiang, 2000; Sasaki et al., 1999; Wijgerde et al., 2002).

[1]Institute for Cellular and Molecular Biology, [2]Section of Neurobiology and [3]Institute for Neuroscience, University of Texas at Austin, Austin, TX 78712-0248, USA.

*Present address: Baylor College of Medicine, MSTP Office, Mail Box 528, Houston, TX 77030, USA
†Author for correspondence (e-mail: agarwala@mail.utexas.edu)

Accepted 13 March 2007

Among vertebrates, one of the best-understood examples of the role of HH in patterning is in the ventral spinal cord (Jessell, 2000). Gain- and loss-of-function studies have shown that HH is both necessary and sufficient for cell-fate specification in the spinal cord (Briscoe and Ericson, 2001; Chiang et al., 1996; Zhang et al., 2001). HH is directly required for cell-fate specification and can pattern cell fates at long range (approximately 15-20 cell diameters) (Briscoe et al., 2001; Wijgerde et al., 2002).

A role for HH signaling in the regulation of cell affinities has been found in the fly wing imaginal disc and abdominal ectoderm (Blair and Ralston, 1997; Lawrence et al., 1999; Rodriguez and Basler, 1997). In each tissue, differential HH signaling creates two compartments that display distinct and inheritable affinities. Thus, cells of a compartment and their lineal relatives cohere with each other and do not intermix with those of the other compartment. As a result, the compartments become separated by a sharp, lineage restriction boundary exhibiting signaling properties (Blair, 1992; Garcia-Bellido et al., 1973; Lawrence et al., 1999; Morata and Lawrence, 1975). These results implicate HH signaling in the establishment of tissue boundaries and in the maintenance of a spatially coherent pattern (Dahmann and Basler, 1999). A loss of spatial organization has also been reported in several HH-pathway mutants in mouse (*Shh*$^{-/-}$;*Gli3*$^{-/-}$, *Smo*$^{-/-}$;*Gli3*$^{-/-}$, *Gli2*$^{-/-}$;*Gli3*$^{-/-}$) and chick (e.g. the *talpid*^{2} mutant) (Agarwala et al., 2005; Bai et al., 2004; Litingtung and Chiang, 2000; Wijgerde et al., 2002). Recently, HH signaling has also been implicated in the maintenance of orthogonal signaling centers in the vertebrate limb and in the midbrain-hindbrain boundary (MHB) of the neural tube (Aoto et al., 2002; Blaess et al., 2006; Khokha et al., 2003). However, whether the regulation of boundaries is a general feature of HH action among vertebrates is not yet known.

In this study, we analyzed the role of HH signaling in the chick midbrain, where stripes of cell fates (midbrain arcs) develop parallel to the rFP source of *SHH* (Agarwala et al., 2001; Sanders et al., 2002). In vivo misexpression studies have shown that ectopic SHH

can recapitulate the entire midbrain pattern of cell fates in a concentration-dependent manner (Agarwala and Ragsdale, 2002; Agarwala et al., 2001). No ventral cell fates remain in the *Shh*$^{-/-}$ mouse midbrain by embryonic day (E)11.5, when the entire midbrain exhibits a dorsal phenotype (Blaess et al., 2006; Fedtsova and Turner, 2001). Although these studies demonstrate the importance of SHH in the developing midbrain, they do not permit a precise cellular and molecular analysis of the role of HH signaling in establishing midbrain pattern. Nor do they elucidate the physical nature of the HH signal; for example, its range (short or long), mode (direct or indirect), timing or duration of action.

To address these issues, we perturbed HH function in the ventral midbrain by in vivo misexpression of *Ptc1*$^{\Delta loop2}$, a mutated form of PTC1 that has been used previously to successfully block HH signaling (Briscoe et al., 2001; Kiecker and Lumsden, 2004). We show that HH is directly required for cell-fate specification within columns of midbrain cells, which are cytoplasmically connected and likely to be clonally related (Noctor et al., 2001). HH signaling acts at long range (approximately 31 cell diameters) at Hamburger and Hamilton (H&H) stage 13, when cell-fate specification is complete at the lateral periphery of the ventral midbrain (Hamburger and Hamilton, 1951). Beyond this time, continued dependence upon HH is only seen within lateral regions of the rFP and cell fates associated with it. Our results also suggest that the blockade of HH signaling increases cell proliferation and inhibits differentiation within the midbrain. Finally, HH is required for the spatial organization of midbrain cell types and for the maintenance of the boundaries of the midbrain. Perturbations of HH signaling thus result in the admixture of midbrain cells with each other and with cells from juxtaposed tissues.

MATERIALS AND METHODS

Chick embryos

Fertilized Leghorn eggs (Ideal Poultry, Texas) were incubated at 38°C in a forced-draft humidified chamber. Embryos were staged according to Hamburger and Hamilton (Hamburger and Hamilton, 1951).

Expression vectors

Embryos were electroporated with either enhanced green fluorescent protein (*EGFP*; EFX-EGFP), *Ptc1*$^{\Delta loop2}$ (pCIG-*Ptc1*$^{\Delta loop2}$) or *SHH* (XEX-SHH)-containing expression vectors. The construction of *Ptc1*$^{\Delta loop2}$ and XEX-SHH has been described previously (Agarwala and Ragsdale, 2002; Agarwala et al., 2001; Briscoe et al., 2001). The second large extracellular loop of mouse *Ptc1* (also known as *Ptch1* – Mouse Genome Informatics) (corresponding to amino acids 793-998), which normally binds the HH ligand, has been deleted in the *Ptc1*$^{\Delta loop2}$ construct. *Ptc1*$^{\Delta loop2}$ can thus maintain a constitutive blockade on SMO, acting as a dominant-negative regulator of HH signaling (Briscoe et al., 2001). The EFX-EGFP construct was created by ligating the *Bam*HI-*Not*I fragment (800 bp) of pEGFPN1 (Clontech) into the plasmid EFX3C (Agarwala et al., 2001).

In ovo electroporation

DNA (1-3 μg/μl) was electroporated into H&H stages 6-20 embryos according to previously established protocols (Agarwala and Ragsdale, 2002; Agarwala et al., 2001; Momose et al., 1999). Electroporated embryos were returned to the incubator for 1-7 days prior to collection for further analyses. Only 20% of the embryos electroporated between H&H stages 6-8 survived to E5.

In situ hybridization

Embryos were harvested between E3 and E8, and were then immersion-fixed in 4% paraformaldehyde. Digoxigenin (DIG)- or Fluorescein-conjugated antisense riboprobes were prepared from cDNAs for class III β-tubulin, cyclin B2, cyclin D1, *EVX1*, *FOXA2*, *GLI2*, *FGF8*, *ISL1*, *LMX1B*, *NKX2.2*, *OTX2*, *PAX6*, *PAX7*, *PHOX2A*, *PTC1*, *SERRATE1*, *SHH*, *TH* and *WNT1*, and from mouse *Ptc1*. The antisense riboprobe for EGFP was generated from pBS-EGFP, constructed by subcloning the *Bam*HI-*Not*I fragment of pEGFPN1 (Clontech) into the bluescript plasmid (Stratagene). One- or two-color whole-mount in situ hybridizations were conducted according to published protocols (Agarwala and Ragsdale, 2002; Agarwala et al., 2001).

Cell-death assay

Whole-mount cell-death assays were carried out on E5 embryos using previously published protocols (Agarwala et al., 2005; Yamamoto and Henderson, 1999) (see also T. A. Sanders, PhD thesis, University of Chicago, 2001).

Midbrain explants

For explant cultures, embryos were electroporated as usual with EFX-EGFP or pCIG-*Ptc1*$^{\Delta loop2}$. Midbrain explants were prepared as previously published with either: (a) an attached dorsal midbrain; (b) no dorsal midbrain; or (c) no dorsal mid- or hind-brain (Agarwala and Ragsdale, 2002). Prepared explants were cultured for 3 days prior to harvesting.

Bromodeoxyuridine labeling

Bromodeoxyuridine [BrdU; 1 μl; 15 mg/ml (50 μM) in PBS; Sigma] was intravenously injected into E5 embryos electroporated at H&H stage 10. Injected embryos were incubated for 30 minutes before fixation. In situ hybridization and the detection of BrdU labeling were combined according to established protocols (Agarwala et al., 2001) (see also T. A. Sanders, PhD thesis, University of Chicago, 2001).

Whole-cell current-clamp recordings

Embryos were explanted at H&H stage 10 as described above and neuronal progenitors were visualized using infrared DIC microscopy (Zeiss Axioscope 2) and a Dage-MTI Newvicon tube camera. Whole-cell current-clamp recordings were made at room temperature using somatic patch pipettes with open tip resistances of 2-4 MΩ. Alexa-Fluor 488 (30 μM) was added to the internal solution, which was made according to published protocols (Scott et al., 2005). Dye-coupled cells were identified by visualizing Alexa-Fluor 488 with fluorescence microscopy (EXFO X-cite 120 light source, Photometrics Cascade 512B camera).

Orientation of photomicrographs

Unless mentioned, images of unilaterally electroporated E5 embryos are presented as whole mounts with rostral to the top and the ventricular surface facing the viewer (open-book view). The electroporated side is presented to the right, the left side serving as a control. Where crucial, the age of electroporation (Fig. 4) or the age of harvest (remaining figures) is provided on the photomicrographs. Embryos bilaterally electroporated with *Ptc1*$^{\Delta loop2}$ are identified with 'bi' on respective panels and EGFP-electroporated controls are provided for comparison. Sections are shown with the ventricular surface at the top and the pial surface at the bottom.

RESULTS

HH signaling is necessary for cell-fate specification in the ventral midbrain

The ventral midbrain pattern is composed of a set of arcuate territories arrayed parallel to the midline (rFP) source of *SHH* (Sanders et al., 2002). These are marked by the gene expression of *PHOX2A* and tyrosine hydroxylase (*TH*) in the most medial arc (arc 1), and more laterally (at a distance from the *SHH* source) by the expression of *NKX2.2*, *PAX6* and *EVX1* (Fig. 1A,F,G and data not shown) (Agarwala and Ragsdale, 2002). We determined that the *SHH* source and the midbrain arc pattern were not perturbed by control electroporations of EGFP (Fig. 1A). The rFP markers *SHH* and *FOXA2* (*HNF3β*) are transcriptional targets of HH signaling in the midbrain (Agarwala et al., 2001), and were suppressed by *Ptc1*$^{\Delta loop2}$ electroporations (Fig. 1B; Fig. 4D). *Ptc1*$^{\Delta loop2}$ misexpression also prevented the correct specification of all ventral midbrain cell fates, resulting in their re-specification to more dorsal (e.g. *PAX7*+) fates (Fig. 1C, Fig. 4G,H, Fig. 6A). We noted a

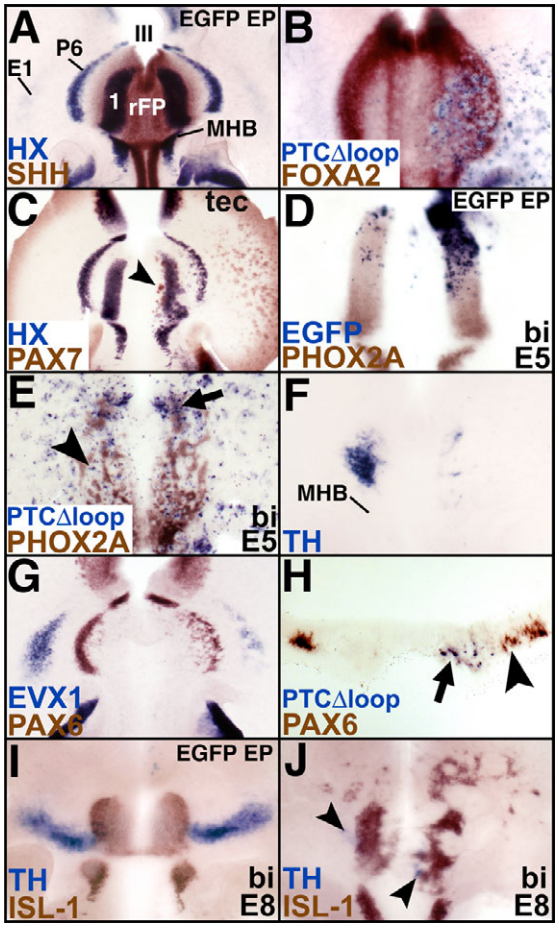

Fig. 1. HH signaling is necessary for cell-fate specification in the ventral midbrain. For orientation and embryonic ages, see Materials and methods. (**A**) At E5, *EGFP*-electroporated (right side) controls do not show disruptions in the rostral floor plate (rFP; *SHH*+, brown) or in midbrain arc pattern formation. Midbrain arcs are marked by the homeobox (HX, blue) gene expression of *PHOX2A* in the first arc (1), *PAX6* (P6) and *EVX1* (E1). (**B**) Blockade of *FOXA2* (brown) expression following unilateral $Ptc1^{\Delta loop2}$ (blue) electroporation (right side). (**C**) Re-specification of ventral cell fates (marked by HX genes, blue) into dorsal (*PAX7*+, brown, arrowhead) cell fates. (**D**,**E**). Blockade and bi-directional spread of *PHOX2A*+ (brown) oculomotor complex neurons following bilateral electroporation (E) of $Ptc1^{\Delta loop2}$ (blue). Compare E with *EGFP*-electroporated controls (D). D and E are photographed at the same magnification. (E) Note the lack (caudally, arrowhead) of overlap between *PHOX2A* and $Ptc1^{\Delta loop2}$ transgene expression. Rostral cells (arrow) have extinguished their requirement for HH signaling by this stage (see text). (**F**,**G**) Reduced expression and spread of tyrosine hydroxylase (F, dopaminergic neurons), *PAX6* (G, brown) and *EVX1* (G, blue) following unilateral HH blockade. (**H**) Cross-section demonstrating the non-autonomous spread of *PAX6*+ (brown, arrowhead) cells following unilateral $Ptc1^{\Delta loop2}$ (blue) electroporation. Note the presence of ectopic PAX6+/$Ptc1^{\Delta loop2}$+ cells (arrow, see text). (**I**,**J**) E8 whole mounts electroproated at H&H stage 10, demonstrating that, compared to EGFP controls (I), cell spread following HH blockade (J) increases with time (compare with the E5 brains in D and E) and is multidirectional. Blue, *TH* (arrowheads); brown, *ISL1*+ motor neurons; 1, first arc; III, third ventricle; bi, bilateral electroporation; E1, *EVX1*; EP, electroporated; P6, *PAX6*; HX, homeobox expression of *PHOX2A*, *PAX6*, *EVX1*; MHB, midbrain-hindbrain boundary; rFP, rostral floor plate; TH, tyrosine hydroxylase; tec, tectum.

suppression of the *PHOX2A*+ oculomotor neurons, midbrain dopaminergic (*TH*+) neurons, as well as the territories (*NKX2.2*+, *PAX6*+, *EVX1*+) specified at a distance from the *SHH* source (Fig. 1D-G and data not shown). Taken together with our previous work, these results suggest that HH signaling is both necessary and sufficient for cell-fate specification in the ventral midbrain and can act directly at a distance to specify midbrain cell fates (Agarwala and Ragsdale, 2002; Agarwala et al., 2001).

HH blockade results in cell spread and in a disrupted midbrain arc pattern

In the fly wing and abdomen, perturbations of HH signaling result in abnormal cell movements due to altered adhesiveness of cells (Blair and Ralston, 1997; Lawrence et al., 1999; Rodriguez and Basler, 1997). An increased spread of cells was also noted within the ventral midbrain following $Ptc1^{\Delta loop2}$ electroporations (compare Fig. 1D and 1E; Fig. 1E-J). This increased scatter was non-autonomous (e.g. Fig. 1E,H), multidirectional, increased dramatically over time (Fig. 1, compare I,J with D,E) and affected progenitors as well as differentiated neurons (see Fig. S1 in the supplementary material). As a result of this scatter, a spatially coherent midbrain arc pattern could not be formed following $Ptc1^{\Delta loop2}$ electroporations (Bai et al., 2004; Blair and Ralston, 1997; Lawrence et al., 1999; Wijgerde et al., 2002).

HH signaling inhibits proliferation and induces neuronal differentiation in the midbrain

HH signaling is known to accelerate progression through the cell cycle in many model systems (Duman-Scheel et al., 2002; Kenney and Rowitch, 2000; Roy and Ingham, 2002). By contrast, we found that the expression of known cell cycle targets of HH signaling (cyclin B2, a marker of G2/M transition; and cyclin D1, a marker of G1/S transition), as well as BrdU labeling (marking the S phase of the cell cycle) all indicated greatly increased numbers of neuronal progenitors following $Ptc1^{\Delta loop2}$ electroporation (Fig. 2A-D) (Masai et al., 2005). Concomitant to the increased proliferation was a reduction in the number of differentiated neurons demonstrated by the reduced thickness of the mantle layer (Fig. 2C,D, double-headed arrow) and reduced class III β-tubulin expression (Fig. 2E, inset). TUNEL labeling indicated no significant differences in cell death between $Ptc1^{\Delta loop2}$ and *EGFP*-electroporated midbrains (see Figs S2 and S3 in the supplementary material).

To discount the possibility that the altered midbrain proliferation and differentiation was due to a peculiarity of the $Ptc1^{\Delta loop2}$ construct itself, we misexpressed *SHH* and found that cyclin D1 mRNA was severely reduced in both the ventral and dorsal midbrain (Fig. 2F,G and see Fig. S4 in the supplementary material) (Guerrero and Ruiz i Altaba, 2003; Thibert et al., 2003). Finally, we compared the total size of midbrains electroporated at H&H stage 9 with either *SHH* or $Ptc1^{\Delta loop2}$ and found that the *SHH*, but not the $Ptc1^{\Delta loop2}$ electroporated midbrains displayed a massive (>50%, in some cases) reduction in size (Fig. 2H). Taken together, these results are consistent with a role for HH signaling in the midbrain in suppressing proliferation and inducing differentiation (Bai et al., 2004; Masai et al., 2005; Wijgerde et al., 2002).

HH blockade reveals a cortex-like radial organization of the ventral midbrain neurepithelium

Following HH blockade, the expression of appropriate midbrain cell-fate determinants (e.g. *FOXA2*, *PHOX2A*) was not only blocked cell-autonomously within cells expressing the $Ptc1^{\Delta loop2}$

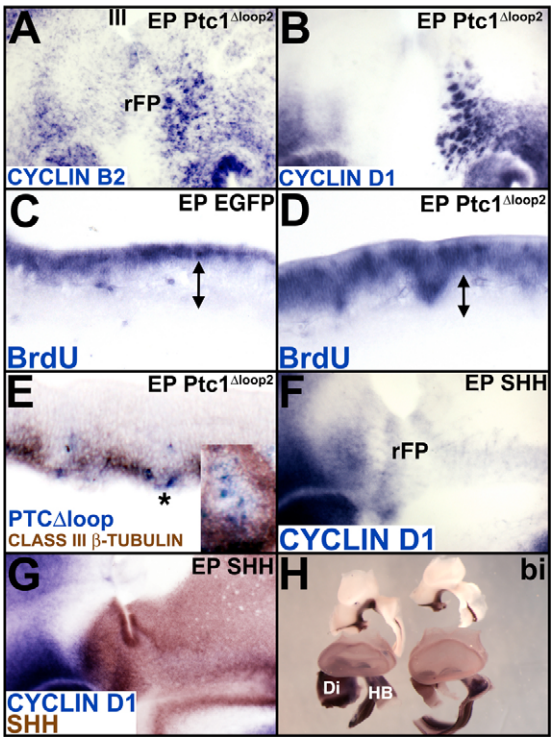

Fig. 2. HH blockade prevents differentiation and promotes proliferation in the ventral midbrain. (**A**,**B**) Increased cyclin B2 (A) and cyclin D1 (B) expression following unilateral misexpression of *Ptc1*$^{\Delta loop2}$. (**C**) BrdU labeling shown in a cross-section through an *EGFP*-electroporated embryo, in which it is confined to proliferating cells of the ventricular layer. (**D**) Massive increase in BrdU labeling (blue) following *Ptc1*$^{\Delta loop2}$ electroporation. Note that the increased thickness of the ventricular layer is associated with a reduction of the mantle layer, where differentiated neurons normally reside (compare double-headed arrows in C and D, which were photographed at the same magnification). (**E**) Cross-section through the ventral midbrain of a *Ptc1*$^{\Delta loop2}$-electroporated embryo, showing a reduction in class III β-tubulin expression (brown, asterisk) following HH blockade. (E, inset) Whole-mount view of the cross-section in E. (**F**,**G**) *SHH* (brown) overexpression results in reduced cyclin D1 (blue) expression. The same embryo is presented in F (before) and G (after) the detection of *SHH*. (**H**) Embryos bilaterally electroporated with either *SHH* (light embryos, upper) or *Ptc1*$^{\Delta loop2}$ (dark embryos, lower) at H&H stage 9. Note the reduced size of *SHH*-electroporated embryos compared with *Ptc1*$^{\Delta loop2}$-electroporated embryos. Embryos are shown in sagittal view, with rostral to the left. III, third ventricle; bi, bilateral electroporation; Di, diencephalon; EP, electroporated; HB, hindbrain; rFP, rostral floor plate.

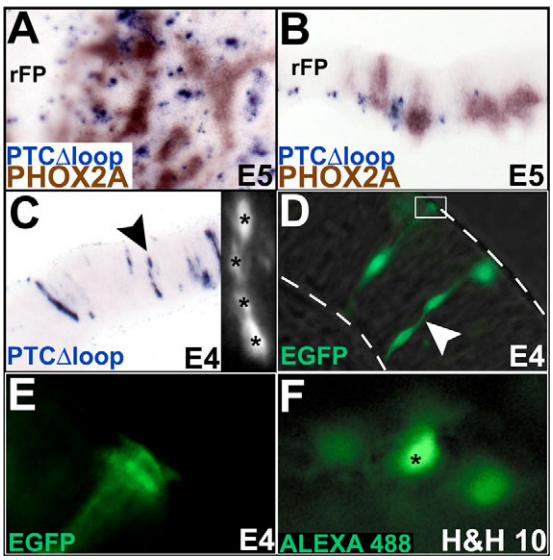

Fig. 3. *Ptc1*$^{\Delta loop2}$ affects cell-fate specification in a radial manner. (**A**) 'Haloes' of PHOX2A-negative/*Ptc1*$^{\Delta loop2}$-negative (uncolored) cells surround *Ptc1*$^{\Delta loop2}$+/PHOX2A-negative (blue) cells. (**B**) Cross-section through whole-mount shown in A, demonstrating that the 'haloes' are columns of PHOX2A-negative/*Ptc1*$^{\Delta loop2}$-negative cells radially associated with more-pially located *Ptc1*$^{\Delta loop2}$+ cells. (**C**) *Ptc1*$^{\Delta loop2}$-electroporated embryos at E4 display midbrain columns in cross-section. (C, inset) Magnified view of a single column of cells (indicated by arrowhead). Individual cells are marked by asterisks. (**D**) Cross-section through an E4 embryo electroporated with low concentrations of *EGFP*, displaying bipolar-radial glia-like midbrain progenitors. Note that, when multiple cells are present in a single column, they are cytoplasmically continuous (arrowhead). (**E**) Close-up of boxed area in D, highlighting the radial glial-like morphology of the midbrain progenitors, including the presence of end-feet at the ventricular surface. (**F**) Demonstration of dye-coupling through gap junctions among three ventral midbrain cells following the injection of Alexa-Fluor 488 into the central cell (*). H&H stage 10 explant presented in whole-mount view (rostral is to the top and ventricular surface faces the viewer; orientation is the same as in Fig. 1A). Each cell is approximately 7.5 μm across and the cells are spaced approximately 5 μm apart. The central cell is ventricular with respect to the other two cells. H&H, embryonic stages according to Hamburger and Hamilton (Hamburger and Hamilton, 1951); rFP, rostral floor plate.

(mouse *Ptc1*) transgene, but also in 'haloes' immediately surrounding the *Ptc1*$^{\Delta loop2}$+ cells (Fig. 3A; Fig. 1B,E). In E5 cross-sections, these 'haloes' (cells that did not express spatially appropriate HH-target fates despite appearing *Ptc1*$^{\Delta loop2}$ negative), were organized into 'columns' of cells that spanned the ventricular-pial (radial) axis and were radially aligned with pially located *Ptc1*$^{\Delta loop2}$+ cells (Fig. 3B).

This columnar organization has not yet been described in the midbrain. However, it bore a remarkable resemblance to the neocortex, where cortical columns emerge to form a lineal relationship between neuronal precursors (radial glia) and their descendants as the latter colonize the cortical plate along the radial axis (Chenn and McConnell, 1995; Kriegstein and Noctor, 2004).

We next determined whether midbrain columns were the result of HH blockade or a normal feature of midbrain organization. For this purpose, we shifted our analysis to E4, when the midbrain neurepithelium is predominantly composed of undifferentiated precursors and HH-blockade-mediated perturbation of proliferation and differentiation does not add additional complexity (Fig. 2A-E).

Columns of electroporated cells spanning the ventricular-pial axis could be seen in *Ptc1*$^{\Delta loop2}$-electroporated embryos at E4 (Fig. 3C). A similar columnar organization was seen in midbrains electroporated with low concentrations of *EGFP* (0.2 μg/μl) to yield only a few isolated EGFP+ cells per brain (Fig. 3D,E). Thus, HH blockade neither induced nor disrupted the columnar organization of the ventral midbrain. Notably, the EGFP+ cells displayed the characteristic morphology of radial glial/neuronal precursors (bipolar cells spanning the midbrain ventricular-pial axis and exhibiting apical and basal processes with end-feet) (Fig. 3E and

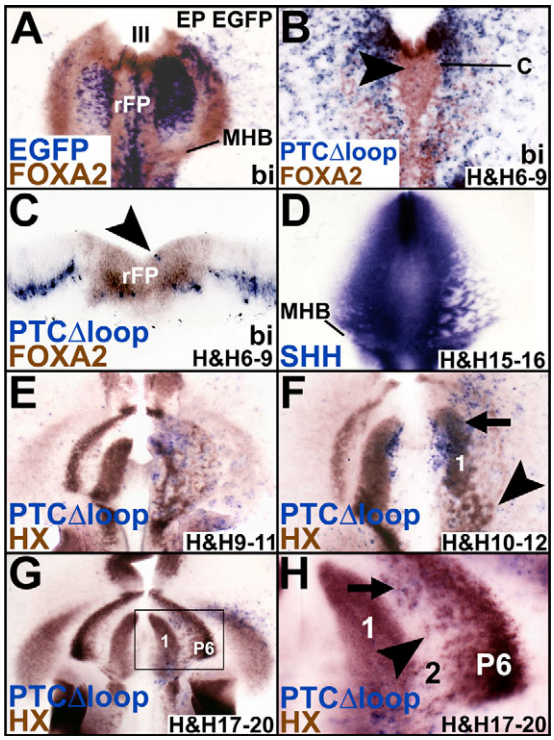

Fig. 4. Spatiotemporal regulation of HH requirement in the ventral midbrain. (**A**) Bilateral EGFP (blue) misexpression does not perturb the expression of rFP genes (*FOXA2*, brown). (**B**,**C**) Caudal-medial and lateral, but not antero-medial (arrowhead), regions of the rFP (*FOXA2*+, brown) can be disrupted following bilateral electroporation of *Ptc1*$^{\Delta loop2}$ (blue) at H&H stages 6-9. (C) Cross-section of B at the level indicated by the line in B. (A-C) Note the meager number of *Ptc1*$^{\Delta loop2}$+ cells at the midline (arrowheads, B,C) compared with controls (A). (**D**) HH blockade disrupts lateral rFP specification at H&H stages 15-16. (**E**) E6 embryo electroporated with *Ptc1*$^{\Delta loop2}$ (blue) between H&H stage 9 and 11, demonstrating the uniform blockade of cell-fate specification in all midbrain arcs, assayed by HX gene expression (brown). Note the extensive cell mixing and disruption of the arc pattern. (**F**) Greater caudal perturbation of the *PHOX2A*+ (1, brown, arrowhead) first arc following *Ptc1*$^{\Delta loop2}$ electroporation (blue) at H&H stages 10-12. The rostral expression of *PHOX2A* (arrow) is largely unaffected despite the higher bilateral expression of the *Ptc1*$^{\Delta loop2}$ transgene in this region. (**G**) E6 embryo electroporated between H&H stages 17 and 20, demonstrating that midbrain cell fates (brown) are independent of HH signaling, except in lateral regions of the rFP and cells associated with it (e.g. arc 2). (**H**) Close-up of boxed area in G, demonstrating that midbrain progenitors within the lateral region of the rFP and the cells associated with it (e.g. arc 2; 2) can be re-specified to more-dorsal (*PAX6*+) cell fates in association with *Ptc1*$^{\Delta loop2}$+ cells (arrow). In addition, dorsal cells (*PAX6*+) can move into this region non-autonomously (arrowhead). 1, first arc; 2, arc 2; III, third ventricle; bi, bilateral electroporation; EP, electroporated; P6, *PAX6*; H&H, embryonic stages according to Hamburger and Hamilton (Hamburger and Hamilton, 1951); HX, homeobox expression of *PHOX2A*, *PAX6*, *EVX1*; MHB, midbrain-hindbrain boundary; rFP, rostral floor plate.

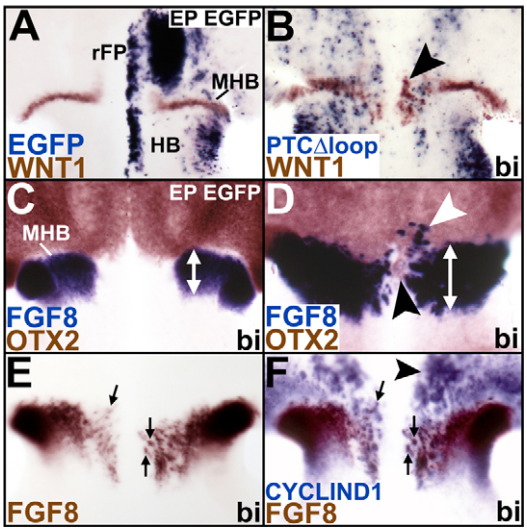

Fig. 5. Disruption and cell mixing at the chick MHB following HH blockade. (**A**,**B**) Unlike EGFP controls (A), bilateral electroporation of *Ptc1*$^{\Delta loop2}$ (blue; B) disrupts *WNT1* (brown, arrowhead) expression at the MHB. (**C**,**D**) Unlike controls (C), HH blockade (D) results in the broadening of *FGF8* expression at the MHB (blue; compare the length of the double-headed arrows in C and D). (D) Note the ectopic mixing of *FGF8*+ (white arrowhead) and *OTX2*+ (brown, black arrowhead) cells. C and D were photographed at the same magnification. (**E**,**F**) Increased cyclin D1 expression within the MHB following bilateral *Ptc1*$^{\Delta loop2}$ electroporations. E and F are photographs of the same embryo demonstrating that all *FGF8*+ cells (arrows, brown) are also cyclin D1+. However, all ectopic cyclin D1+ (arrowhead) cells are not *FGF8*+ (see Fig. 2A, left side, for normal cyclin D1+ expression). bi, bilateral electroporation; EP, electroporated; HB, hindbrain; MHB, midbrain-hindbrain boundary; rFP, rostral floor plate.

data not shown) (Malatesta et al., 2003; Noctor et al., 2001). Furthermore, when multiple EGFP+ cells were present within a single midbrain column, they were cytoplasmically connected (Fig. 3D, arrowhead). Cytoplasmic connections (via gap junctions) among clonal relatives are a feature of cortical columns and have been detected in dye-coupling experiments (Noctor et al., 2001). Indeed, single-cell injections in midbrain explants at H&H stage 10 with Alexa-Fluor 488 (which crosses gap junctions, but does not diffuse across cell membranes) resulted in the instantaneous labeling of up to three cells, demonstrating the presence of gap junctions among midbrain progenitors (n=5; Fig. 3F).

A detailed description of midbrain columns will be published elsewhere (R.D.B. and S.A., unpublished observations). We propose that columns of *Ptc1*$^{\Delta loop2}$ negative cells that are radially associated with *Ptc1*$^{\Delta loop2}$+ cells are unable to express appropriate HH-target fates because they divide and differentiate under reduced HH conditions. Such conditions could be created by the cytoplasmic inheritance of low/undetectable levels of *Ptc1*$^{\Delta loop2}$ (cell-autonomous) or due to the transfer of small inhibitory molecules (e.g. provitamin D3) among neuronal precursors via gap junctions (Bijlsma et al., 2006). For precision, we have described the radial effects of *Ptc1*$^{\Delta loop2}$ electroporations as being 'radially associated' or 'associated' with *Ptc1*$^{\Delta loop2}$+ cells, rather than being cell-autonomous or non-autonomous.

Spatiotemporal regulation of ventral midbrain patterning by HH

We next determined the spatiotemporal sequence in which midbrain cell fates extinguished their dependence upon HH signaling. Compared with *EGFP*-electroporated controls (Fig. 4A, Fig. 5A), very few *Ptc1*$^{\Delta loop2}$+ cells were seen within the medial region of the

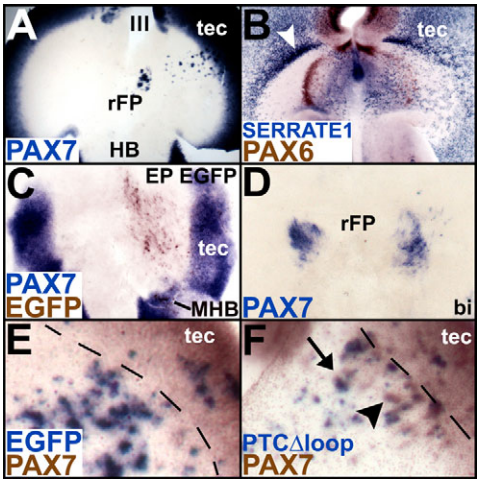

Fig. 6. HH blockade leads to a disruption of the DV boundary. (**A**) Ectopic *PAX7* expression in the ventral midbrain after HH blockade. (**B**) Serrate 1 expression (blue), which is normally confined to the dorsal midbrain (tec) and to a thickening at the DV boundary (arrowhead), is perturbed in $Ptc1^{\Delta loop2}$ electroporations. (**C**) Absence of *PAX7*+ (blue) cells in the ventral midbrain of *EGFP* (brown)-electroporated explants. Note the presence of *PAX7* (blue) expression in the tectum (tec). (**D**) Bilateral $Ptc1^{\Delta loop2}$ electroporation induces ectopic *PAX7* expression in ventral midbrain explants with no associated tectal tissue. (**E**) EGFP misexpression (blue) near the DV boundary (broken line) fails to perturb *PAX7* expression (brown). (**F**) $Ptc1^{\Delta loop2}$ misexpression (blue) near the DV boundary (broken line) induces ectopic *PAX7*+ (brown) cells, some non-autonomously (arrowhead). Arrow points to the upregulation of *PAX7* in association with $Ptc1^{\Delta loop2}$ misexpression. III, third ventricle; bi, bilateral electroporation; EP, electroporated; HB, hindbrain; MHB, midbrain-hindbrain boundary; rFP, rostral floor plate; tec, tectum.

rFP in bilateral electroporations (Fig. 4B,F, Fig. 5B) (Briscoe et al., 2001; Wijgerde et al., 2002). When they did appear at the midline, they could only suppress *SHH* or *FOXA2* gene expression along the caudal (near the MHB), but not anterior (Fig. 4B, arrowhead), midline of rFP between H&H stages 6-11 (Fig. 4B,C, Fig. 7A). By sharp contrast, floor plate markers (*SHH*, *FOXA2*) could be blocked in lateral regions of the rFP in electroporations conducted between H&H stages 15-20 (Fig. 4D, Fig. 7A-C).

In contrast to the rFP, $Ptc1^{\Delta loop2}$ misexpression between H&H stages 8-13 (n>40) resulted in the uniform blockade of all arc-specific cell fates throughout the mediolateral (ML) axis of the ventral midbrain (Fig. 4E,F). Although ML differences in specification were not noticed across the midbrain arcs following HH blockade during this time, cell-fate specification was more severely affected near the MHB compared with more rostral regions, particularly within the medial arc territory (7/10 embryos; Fig. 4F).

In electroporations beyond H&H stage 13, only cell fates associated with the lateral regions of the rFP and arc 2 (the region between the *PHOX2A* and *PAX6* territories) were affected by HH blockade (Fig. 4G,H and see Fig. S5 in the supplementary material). Intriguingly, this region was marked by the ectopic presence of more lateral (e.g. *PAX6*+) phenotypes occurring both non-autonomously (Fig. 4H, arrowhead) and in radial association with misexpressed $Ptc1^{\Delta loop2}$ (Fig. 4H, arrow). We saw a similar mixed phenotype (radially associated and non-autonomous) throughout the study and interpret these results as a combination of re-specified cell fates to a more dorsal identity (radially associated with $Ptc1^{\Delta loop2}$+ cells) and abnormal cell scatter (non-autonomous; see Discussion).

Our data suggest that the anterior midline rFP was not affected by our manipulations between H&H stages 6 and 20, possibly because they are specified earlier or independent of HH signaling (Patten et al., 2003). HH-mediated specification of the remaining ventral midbrain cell fates occurs in at least three temporal phases (Fig. 7A-C). First, prior to H&H stage 11, the caudo-medial region of the rFP becomes independent of HH signaling (step 1; Fig. 7A). This is followed by most ventral midbrain cell fates becoming independent of HH signaling by H&H stage 13 (step 2; Fig. 7B). Beyond H&H stage 13, only the lateral regions of the rFP and cells associated with it exhibit a dependence upon HH signaling and continue to do so at least until H&H stages 17-20 (step 3; Fig. 7C).

Perturbations of HH signaling result in a disruption of midbrain boundaries

In the fly wing and abdomen, HH perturbations result in a disruption of cell affinities, evident as a spatially disorganized pattern and disrupted compartment boundaries (Fig. 1) (Lawrence et al., 1999). We asked whether midbrain boundary perturbation accompanied the disruption of spatial pattern as well (Aoto et al., 2002; Blaess et al., 2006; Lawrence et al., 1999; Zervas et al., 2005).

The midbrain-hindbrain boundary

$Ptc1^{\Delta loop2}$ misexpression resulted in a broadening of the MHB and a non-autonomous scattering of *WNT1*+ cells that was not seen in control brains (Fig. 5A,B). Strikingly, $Ptc1^{\Delta loop2}$ manipulations resulted in the intermingling of midbrain (*OTX2*+) and MHB/hindbrain cells (*FGF8*+; Fig. 5C,D and see Fig. S6 in the supplementary material). This was accompanied by a dramatic broadening of the *FGF8*+ MHB territory (Fig. 5C,D). The broadening could not be explained by a repression of *OTX2*, an expansion of *GBX2* or the ectopic presence of mis-specified cells (Fig. 5D, Fig. S6 in the supplementary material and data not shown). Instead, the broadening could be attributed to enhanced cell proliferation within the MHB, as demonstrated by the dramatic increase of cyclin D1+/*FGF8*+ cells (Fig. 5E,F). Thus, reduced HH signaling results in an enlarged MHB that is not sharply defined and across which cell-mixing can occur (Vaage, 1969; Zervas et al., 2004).

The dorsoventral boundary

The disruption of the MHB following $Ptc1^{\Delta loop2}$ manipulations prompted us to examine the dorsoventral (DV) boundary. When electroporated with $Ptc1^{\Delta loop2}$, ectopic *PAX7*+ cells, normally confined to the dorsal midbrain, were noticed in the ventral midbrain (Fig. 6A). We also observed that the expression of the DELTA homolog, serrate 1, was disrupted along the DV boundary following $Ptc1^{\Delta loop2}$ electroporations (Fig. 6B).

The presence of *PAX7*+ cells in the ventral midbrain could result from a conversion of ventral midbrain cells to a dorsal fate or from the movement of dorsal cells into the ventral midbrain because of a breach in the signals that normally restrict their admixture. To distinguish between these possibilities, we resorted to an explant system, in which all *PAX7*+ dorsal tissue could be removed prior to electroporation with $Ptc1^{\Delta loop2}$ (Agarwala and Ragsdale, 2002). In *EGFP*-electroporated control explants with or without an intact tectum, no *PAX7*+ cells were ever seen in the ventral midbrain (n=11/11; Fig. 6C and data not shown). When explants prepared without any associated *PAX7*+ tissue (dorsal midbrain and

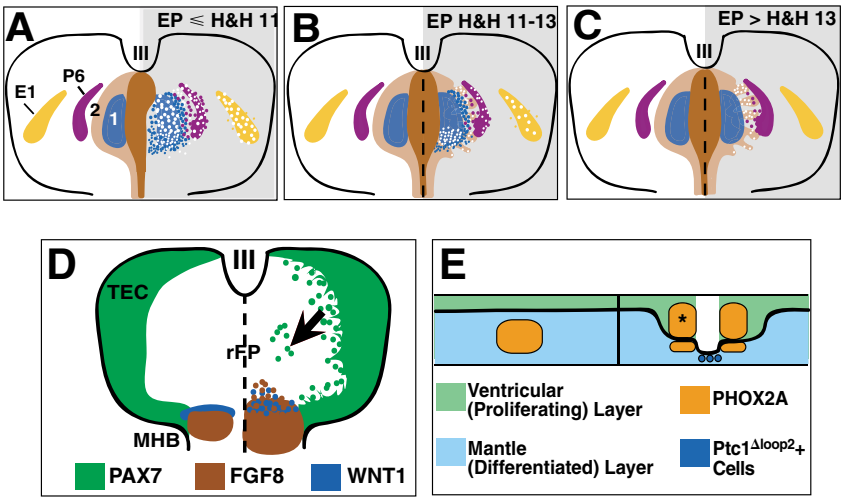

Fig. 7. Summary of HH function in the ventral midbrain. (**A-D**) Whole mounts; (**E**) cross-section. (A-C) A three-step temporal patterning of the ventral midbrain by HH blockade. (A) Electroporation at or before H&H stage 11: anterior-medial rFP patterning is complete or HH-independent. The caudo-medial rFP, lateral rFP and all other midbrain cell fates still require HH signaling for their specification. Increased cell spread is noted. (B) Electroporation at H&H stages 11-13: medial rFP specification is complete. Lateral rFP and arcuate cell fates, represented here by *PHOX2A* (blue), *PAX6* (purple) and *EVX1* (yellow), continue to be specified. The caudo-medial midbrain requires HH signaling for a longer time than does the rostral midbrain. HH is also required for forming a coherent arc pattern. (C) Electroporation after H&H stage 13: midbrain patterning is complete, with the exception of the lateral rFP and cell fates associated with this region (e.g. arc 2). Ectopic cell spread is noted only in this region. (D) HH signaling regulates midbrain boundaries. Disruption of the boundaries of the midbrain results in the non-autonomous spread of *PAX7*+ (green) cells at the DV boundary and of *WNT1*+ (blue) cells and *FGF8*+ (brown) cells at the MHB. Ectopic *PAX7* expression (arrow) is also seen in ventral midbrain progenitors as a result of re-specification into dorsal phenotypes. (E) *PHOX2A* expression, demonstrating that $Ptc1^{\Delta loop2}$ electroporations (right of the vertical line) result in increased cell proliferation (expanded ventricular layer) and in reduced differentiation compared with controls (left of the vertical line). The effects are seen within columns of cytoplasmically connected midbrain cells (white), which line up ventricular to the $Ptc1^{\Delta loop2}$+ cells (blue circles). Non-autonomous cell spread (*) is also seen. 1, first arc; 2, arc 2; III, third ventricle; E1, EVX1; EP, electroporated; P6, *PAX6*; H&H, embryonic stages according to Hamburger and Hamilton (Hamburger and Hamilton, 1951); MHB, midbrain-hindbrain boundary; rFP: rostral floor plate; TEC, tectum.

hindbrain; *n*=4/4) were electroporated with $Ptc1^{\Delta loop2}$, *PAX7*+ cells could be observed within the ventral midbrain, suggesting that some ventral midbrain cells were converted to a dorsal (*PAX7*+) phenotype in the absence of HH signaling (Fig. 6D).

In the absence of any tectum or dorsal hindbrain, the in vitro experiments presented in Fig. 6D cannot definitively rule out the additional possibility of the movement of cells from adjacent tissues, as noted before (Fig. 4G,H, Fig. 5A-D). To resolve this, we resorted to in vivo misexpression of $Ptc1^{\Delta loop2}$ near the DV boundary followed by the simultaneous detection of *PAX7* and the $Ptc1^{\Delta loop2}$ transgene. Ectopic *PAX7*+ cells were not seen near the DV boundary in *EGFP*-electroporated brains (*n*=0/5; Fig. 6E). However, there was always a small number of cells that displayed *PAX7* expression non-autonomously in $Ptc1^{\Delta loop2}$-electroporated brains (*n*=7/7; Fig. 6F). Taken together, our results are consistent with both a transformation of ventral midbrain cell fates to dorsal fates and with a non-autonomous movement of dorsal cells into the ventral midbrain due to an MHB-like disruption of the DV boundary.

DISCUSSION

In this study, we focused on the cellular and molecular mechanisms governed by HH signaling in the ventral midbrain and summarize our conclusions in Fig. 7. We show that HH acts within columns of cytoplasmically connected midbrain progenitors to directly specify cell fates at a distance (Fig. 7E) (Kriegstein and Noctor, 2004). The specification of HH-target midbrain cell fates is largely complete by H&H stage 13, with a continued requirement for HH signaling beyond this time point only in lateral regions of the rFP and associated cell types (e.g. arc 2; Fig. 7A-C). Interestingly, $Ptc1^{\Delta loop2}$ electroporations result in increased cell proliferation and reduced differentiation, closely resembling the size regulation in $Gli2^{-/-}$;$Gli3^{-/-}$ and $Smo^{-/-}$;$Gli3^{-/-}$, but not $Shh^{-/-}$, mice (Fig. 7E) (Bai et al., 2004; Litingtung and Chiang, 2000; Wijgerde et al., 2002). Finally, HH signaling is required for the correct spatial patterning of midbrain cell types and for the integrity of the boundaries of the midbrain (MHB, DV boundary; Fig. 7D).

The range of HH action in the midbrain

We determined that direct HH signaling was required at the lateral edge of the ventral midbrain and that this requirement was extinguished by H&H stage 13 (Figs 1, 4). The restriction of *PAX7* expression to the dorsal midbrain by HH is a measure of the range of HH signaling (Ericson et al., 1996; Wijgerde et al., 2002). The distance between the lateral limit of the *SHH* source and the ventral limit of the *PAX7* domain in the midbrain at H&H stage 10, when midbrain patterning is ongoing, is approximately 180 μm. Based on our dye-coupling experiments (Fig. 3F), the average cell diameter of midbrain neurepithelial cells at H&H stage 10 is approximately 7.5 μm (range 5-10 μm; data not shown). Thus, at H&H stage 10, the SHH signal must travel up to approximately 24 cell diameters to influence cell fates at the lateral periphery of the ventral midbrain. This distance increases to approximately 31 cell diameters at H&H stage 13, which is only 1.5 times the distance of 12-20 cell diameters traversed by the HH signal in the fly wing, vertebrate limb and spinal cord (Briscoe et al., 2001; Ericson et al., 1996; Harfe et al., 2004; Tabata and Takei, 2004; Wijgerde et al., 2002). Thus, despite the ultimately different sizes of the midbrain and spinal cord, the problem of getting the HH signal across long distances is circumvented by accomplishing midbrain cell-fate specification relatively early, when the midbrain size is small and comparable to the spinal cord. The role of continued *SHH* expression beyond this time point is not known, although cell survival, axon guidance, dorsal patterning and size regulation are possible functions (Blaess et al., 2006; Ishibashi and McMahon, 2002).

HH signaling regulates cell cycle and differentiation in the developing midbrain

Blockade and overexpression experiments demonstrate that HH regulates midbrain size by preventing cell proliferation and by inducing differentiation with no significant alterations in cell survival (Fig. 2). Although midbrain size regulation in the chick midbrain following *Ptc1*$^{\Delta loop2}$ manipulations differs from that reported for the *Shh*$^{-/-}$ mouse, it strongly resembles the phenotype of the mouse *Gli2*$^{-/-}$;*Gli3*$^{-/-}$ and *Smo*$^{-/-}$;*Gli3*$^{-/-}$ spinal cords, in which no HH signaling is possible (Bai et al., 2004; Blaess et al., 2006; Chiang et al., 1996; Ishibashi and McMahon, 2002; Wijgerde et al., 2002). Why size regulation differs between these two sets of mice is not clear, but may depend upon the levels of GLI repressor present in each manipulation (Cayuso et al., 2006) and also upon the ligand-independent interactions between the cell cycle and HH pathway members (Barnes et al., 2005). Interestingly, HH signaling in the retina and cerebellar granule cells regulates multiple aspects of proliferation and differentiation (e.g. G1–S transition, cell-cycle exit and neuronal differentiation) (Duman-Scheel et al., 2002; Pons et al., 2001; Wechsler-Reya and Scott, 1999). Thus, whether HH is a positive or a negative regulator of size may depend upon the cellular context and the level of the HH signaling cascade at which a given HH perturbation is targeted (Masai et al., 2005; Neumann, 2005).

HH blockade results in increased cell scatter and disrupts the midbrain arc pattern

Increased cell scatter and a disruption of the arc pattern followed *Ptc1*$^{\Delta loop2}$ electroporation in the ventral midbrain (Fig. 1, Fig. 4G,H). Similar disruptions in spatial patterning have also been seen following HH perturbations in multiple systems in the fly, mouse and chick (Agarwala et al., 2005; Bai et al., 2004; Lawrence, 1997; Litingtung and Chiang, 2000; Wijgerde et al., 2002). In the chick midbrain, spatially inappropriate cell fates appeared both in radial association with *Ptc1*$^{\Delta loop2}$+ cells as well as non-autonomously (e.g. Fig. 1H, Fig. 4G,H). Because robust *Ptc1*$^{\Delta loop2}$ transgene was seen at E5-E6 (e.g. Fig. 1B, Fig. 4G), the selective shutdown of transgene expression in subgroups of manipulated cells is an unlikely explanation for the dual phenotype. We noticed that cell-mixing/movement across midbrain boundaries (MHB, DV boundary) following HH blockade invariably occurred in a non-autonomous manner (Figs 5, 6). Thus, a possible explanation for this dual phenotype is that it represents a combination of cell-spread (non-autonomous) and cell-fate re-specification (in radial association with *Ptc1*$^{\Delta loop2}$+ cells).

Previous studies have noted a cell-autonomous, stepwise dorsalization of cell fates and a non-autonomous, stepwise dorsal-to-ventral transformation of cell fates due to a failure of *Ptc1*$^{\Delta loop2}$+ cells to sequester HH (Briscoe et al., 2001). However, in the midbrain, the non-autonomous effects were non-directional, affected progenitors and differentiated neurons, and increased dramatically with time (Fig. 1l and see Fig. S1 in the supplementary material). Thus, we interpret our findings as increased cell spread rather than a dorsal-to-ventral re-specification due to the failure of *Ptc1*$^{\Delta loop2}$ to bind the HH ligand.

HH regulates the boundaries of the midbrain with adjacent tissues

In this study, we show that a consequence of HH blockade in the midbrain is increased cell proliferation, resulting in a broadened MHB across which cell mixing can occur (Kiecker and Lumsden, 2005; Vaage, 1969; Zervas et al., 2005). Recent evidence suggests that, rather than being a single boundary, the MHB may be a compartment flanked by two boundaries, much like the zona limitans intrathalamica (ZLI) in the diencephalon (Kiecker and Lumsden, 2005). The MHB is sharpened over time via the mutual repression of OTX2 and GBX2 (Zervas et al., 2005). Taken together with our observations, these results support a role for HH signaling in sharpening the MHB by inhibiting cell proliferation. Furthermore, although controversial, the MHB is likely to be a lineage-restriction boundary, which, like rhombomere boundaries, is somewhat 'leaky' and permits a limited amount of cell mixing (Fig. 5C,D) (Jungbluth et al., 2001; Zervas et al., 2005). The increased cell mixing noted across the MHB following HH blockade in our experiments therefore suggests a role for HH signaling in limiting such cell mixing. This is corroborated in the *Shh*$^{-/-}$ mouse, in which MHB cells can be found scattered several cell diameters away from the MHB (J.L.F. and S.A., unpublished observations).

The requirement for HH in boundary maintenance is not confined to the MHB. In Fig. 6, we noted that the DV boundary and the accompanying serrate 1 expression are also perturbed as a consequence of HH blockade and result in cell mixing. No patterning properties are ascribed to the midbrain DV boundary yet, but Serrate and Notch-Delta interactions have been implicated in DV patterning in the fly and vertebrate limb and in the establishment of the apical ectodermal ridge, a signaling center at the DV interface (Irvine and Vogt, 1997). We conclude that maintaining the integrity and the signaling properties of boundary regions, and therefore the territorial integrity of the ventral midbrain, is an important function of HH signaling.

Radial patterning and the cell autonomy of HH action within the ventral midbrain

In Fig. 3, we show that the specification of the appropriate cell fates was not only blocked within *Ptc1*$^{\Delta loop2}$+ cells but also in columns of *Ptc1*$^{\Delta loop2}$ negative cells that were radially aligned with them. In *EGFP* electroporations, we show that cells within a single midbrain column can be cytoplasmically continuous, raising the possibility of the transfer of small, undetectable amounts of *Ptc1*$^{\Delta loop2}$ between these cells to block fate specification. In the cortex, lineally related cells occupy similar radial columns and are cytoplasmically connected via gap junctions (Chenn and McConnell, 1995; Noctor et al., 2001). Intriguingly, gap junctions are also found among midbrain progenitors (Fig. 3F). A recent in vitro study has elegantly demonstrated the involvement of PTC1-mediated induction of provitamin D3 in suppressing HH signaling in juxtaposed cells (Bijlsma et al., 2006). This model supports the extracellular transport of provitamin D3 in the non-autonomous blockade of SMO in adjacent cells. However, provitamin D3 is a small molecule (384.6 Da) and could pass through gap junctions from an electroporated cell to its cytoplasmically connected neighbors to block cell-fate specification. Thus, although the radial organization of the midbrain may depend upon the alignment of clonally related cells, their cytoplasmic connections may help explain why they share similar fates following HH blockade.

We thank L. L. Scott and N. L. Golding for help with the patch-clamp experiments; P. Beachy, P. Brickell, J. Briscoe, C. Cepko, D. Cleveland, G. Eichele, C. Fan, C. Goridis, M. Goulding, B. Houston, T. Jessell, J. Lahti, A. Leutz, J. Lewis, C. Logan, A. McMahon, G. Martin, C. Ragsdale, J. Rubenstein, G. Struhl, C. Tabin and M. Wassef for DNA reagents; and C. Ragsdale, J. Fallon, T. Shimogori and C. Chiang for critical reading of the manuscript. This research was supported by a grant from the National Institutes of Health to S.A. and from the University of Texas at Austin start-up funds.

Supplementary material

Supplementary material for this article is available at http://dev.biologists.org/cgi/content/full/134/11/2115/DC1

References

Agarwala, S. and Ragsdale, C. W. (2002). A role for midbrain arcs in nucleogenesis. *Development* **129**, 5779-5788.

Agarwala, S., Sanders, T. A. and Ragsdale, C. W. (2001). Sonic hedgehog control of size and shape in midbrain pattern formation. *Science* **291**, 2147-2150.

Agarwala, S., Aglyamova, G. V., Marma, A. K., Fallon, J. F. and Ragsdale, C. W. (2005). Differential susceptibility of midbrain and spinal cord patterning to floor plate defects in the talpid2 mutant. *Dev. Biol.* **288**, 206-220.

Akiyama, H., Shigeno, C., Hiraki, Y., Shukunami, C., Kohno, H., Akagi, M., Konishi, J. and Nakamura, T. (1997). Cloning of a mouse smoothened cDNA and expression patterns of hedgehog signalling molecules during chondrogenesis and cartilage differentiation in clonal mouse EC cells, ATDC5. *Biochem. Biophys. Res. Commun.* **235**, 142-147.

Alcedo, J., Ayzenzon, M., Von Ohlen, T., Noll, M. and Hooper, J. E. (1996). The Drosophila smoothened gene encodes a seven-pass membrane protein, a putative receptor for the hedgehog signal. *Cell* **86**, 221-232.

Aoto, K., Nishimura, T., Eto, K. and Motoyama, J. (2002). Mouse GLI3 regulates Fgf8 expression and apoptosis in the developing neural tube, face, and limb bud. *Dev. Biol.* **251**, 320-332.

Aza-Blanc, P., Ramirez-Weber, F. A., Laget, M. P., Schwartz, C. and Kornberg, T. B. (1997). Proteolysis that is inhibited by hedgehog targets Cubitus interruptus protein to the nucleus and converts it to a repressor. *Cell* **89**, 1043-1053.

Bai, C. B., Stephen, D. and Joyner, A. L. (2004). All mouse ventral spinal cord patterning by hedgehog is Gli dependent and involves an activator function of Gli3. *Dev. Cell* **6**, 103-115.

Barnes, E. A., Heidtman, K. J. and Donoghue, D. J. (2005). Constitutive activation of the shh-ptc1 pathway by a patched1 mutation identified in BCC. *Oncogene* **24**, 902-915.

Bijlsma, M. F., Spek, C. A., Zivkovic, D., van de Water, S., Rezaee, F. and Peppelenbosch, M. P. (2006). Repression of Smoothened by Patched-dependent (Pro-)vitamin D3 secretion. *PLoS Biol.* **4**, e232.

Blaess, S., Corrales, J. D. and Joyner, A. L. (2006). Sonic hedgehog regulates Gli activator and repressor functions with spatial and temporal precision in the mid/hindbrain region. *Development* **133**, 1799-1809.

Blair, S. S. (1992). Engrailed expression in the anterior lineage compartment of the developing wing blade of Drosophila. *Development* **115**, 21-33.

Blair, S. S. and Ralston, A. (1997). Smoothened-mediated Hedgehog signalling is required for the maintenance of the anterior-posterior lineage restriction in the developing wing of Drosophila. *Development* **124**, 4053-4063.

Briscoe, J. and Ericson, J. (2001). Specification of neuronal fates in the ventral neural tube. *Curr. Opin. Neurobiol.* **11**, 43-49.

Briscoe, J., Chen, Y., Jessell, T. M. and Struhl, G. (2001). A hedgehog-insensitive form of patched provides evidence for direct long-range morphogen activity of sonic hedgehog in the neural tube. *Mol. Cell* **7**, 1279-1291.

Cayuso, J., Ulloa, F., Cox, B., Briscoe, J. and Marti, E. (2006). The Sonic hedgehog pathway independently controls the patterning, proliferation and survival of neuroepithelial cells by regulating Gli activity. *Development* **133**, 517-528.

Chenn, A. and McConnell, S. K. (1995). Cleavage orientation and the asymmetric inheritance of Notch1 immunoreactivity in mammalian neurogenesis. *Cell* **82**, 631-641.

Chiang, C., Litingtung, Y., Lee, E., Young, K. E., Corden, J. L., Westphal, H. and Beachy, P. A. (1996). Cyclopia and defective axial patterning in mice lacking Sonic hedgehog gene function. *Nature* **383**, 407-413.

Dahmann, C. and Basler, K. (1999). Compartment boundaries: at the edge of development. *Trends Genet.* **15**, 320-326.

Dai, P., Akimaru, H., Tanaka, Y., Maekawa, T., Nakafuku, M. and Ishii, S. (1999). Sonic Hedgehog-induced activation of the Gli1 promoter is mediated by GLI3. *J. Biol. Chem.* **274**, 8143-8152.

Duman-Scheel, M., Weng, L., Xin, S. and Du, W. (2002). Hedgehog regulates cell growth and proliferation by inducing Cyclin D and Cyclin E. *Nature* **417**, 299-304.

Ericson, J., Morton, S., Kawakami, A., Roelink, H. and Jessell, T. M. (1996). Two critical periods of Sonic Hedgehog signaling required for the specification of motor neuron identity. *Cell* **87**, 661-673.

Fedtsova, N. and Turner, E. E. (2001). Signals from the ventral midline and isthmus regulate the development of Brn3.0-expressing neurons in the midbrain. *Mech. Dev.* **105**, 129-144.

Garcia-Bellido, A., Ripoll, P. and Morata, G. (1973). Developmental compartmentalisation of the wing disk of Drosophila. *Nat. New Biol.* **245**, 251-253.

Guerrero, I. and Ruiz i Altaba, A. (2003). Development. Longing for ligand: hedgehog, patched, and cell death. *Science* **301**, 774-776.

Hamburger, V. and Hamilton, H. L. (1951). A series of normal stages in the development of the chick embryo. *J. Morphol.* **88**, 49-92.

Harfe, B. D., Scherz, P. J., Nissim, S., Tian, H., McMahon, A. P. and Tabin, C. J. (2004). Evidence for an expansion-based temporal Shh gradient in specifying vertebrate digit identities. *Cell* **118**, 517-528.

Hooper, J. E. and Scott, M. P. (2005). Communicating with Hedgehogs. *Nat. Rev. Mol. Cell Biol.* **6**, 306-317.

Ingham, P. W. and McMahon, A. P. (2001). Hedgehog signaling in animal development: paradigms and principles. *Genes Dev.* **15**, 3059-3087.

Irvine, K. D. and Vogt, T. F. (1997). Dorsal-ventral signaling in limb development. *Curr. Opin. Cell Biol.* **9**, 867-876.

Ishibashi, M. and McMahon, A. P. (2002). A sonic hedgehog-dependent signaling relay regulates growth of diencephalic and mesencephalic primordia in the early mouse embryo. *Development* **129**, 4807-4819.

Jessell, T. M. (2000). Neuronal specification in the spinal cord: inductive signals and transcriptional codes. *Nat. Rev. Genet.* **1**, 20-29.

Jungbluth, S., Larsen, C., Wizenmann, A. and Lumsden, A. (2001). Cell mixing between the embryonic midbrain and hindbrain. *Curr. Biol.* **11**, 204-207.

Kenney, A. M. and Rowitch, D. H. (2000). Sonic hedgehog promotes G(1) cyclin expression and sustained cell cycle progression in mammalian neuronal precursors. *Mol. Cell. Biol.* **20**, 9055-9067.

Khokha, M. K., Hsu, D., Brunet, L. J., Dionne, M. S. and Harland, R. M. (2003). Gremlin is the BMP antagonist required for maintenance of Shh and Fgf signals during limb patterning. *Nat. Genet.* **34**, 303-307.

Kiecker, C. and Lumsden, A. (2004). Hedgehog signaling from the ZLI regulates diencephalic regional identity. *Nat. Neurosci.* **7**, 1242-1249.

Kiecker, C. and Lumsden, A. (2005). Compartments and their boundaries in vertebrate brain development. *Nat. Rev. Neurosci.* **6**, 553-564.

Kriegstein, A. R. and Noctor, S. C. (2004). Patterns of neuronal migration in the embryonic cortex. *Trends Neurosci.* **27**, 392-399.

Lawrence, P. A. (1997). Developmental biology. Straight and wiggly affinities. *Nature* **389**, 546-547.

Lawrence, P. A., Casal, J. and Struhl, G. (1999). The hedgehog morphogen and gradients of cell affinity in the abdomen of Drosophila. *Development* **126**, 2441-2449.

Litingtung, Y. and Chiang, C. (2000). Specification of ventral neuron types is mediated by an antagonistic interaction between Shh and Gli3. *Nat. Neurosci.* **3**, 979-985.

Malatesta, P., Hack, M. A., Hartfuss, E., Kettenmann, H., Klinkert, W., Kirchhoff, F. and Gotz, M. (2003). Neuronal or glial progeny: regional differences in radial glia fate. *Neuron* **37**, 751-764.

Marigo, V., Scott, M. P., Johnson, R. L., Goodrich, L. V. and Tabin, C. J. (1996). Conservation in hedgehog signaling: induction of a chicken patched homolog by Sonic hedgehog in the developing limb. *Development* **122**, 1225-1233.

Masai, I., Yamaguchi, M., Tonou-Fujimori, N., Komori, A. and Okamoto, H. (2005). The hedgehog-PKA pathway regulates two distinct steps of the differentiation of retinal ganglion cells: the cell-cycle exit of retinoblasts and their neuronal maturation. *Development* **132**, 1539-1553.

Momose, T., Tonegawa, A., Takeuchi, J., Ogawa, H., Umesono, K. and Yasuda, K. (1999). Efficient targeting of gene expression in chick embryos by microelectroporation. *Dev. Growth Differ.* **41**, 335-344.

Morata, G. and Lawrence, P. A. (1975). Control of compartment development by the engrailed gene in Drosophila. *Nature* **255**, 614-617.

Neumann, C. J. (2005). Hedgehogs as negative regulators of the cell cycle. *Cell Cycle* **4**, 1139-1140.

Noctor, S. C., Flint, A. C., Weissman, T. A., Dammerman, R. S. and Kriegstein, A. R. (2001). Neurons derived from radial glial cells establish radial units in neocortex. *Nature* **409**, 714-720.

Patten, I., Kulesa, P., Shen, M. M., Fraser, S. and Placzek, M. (2003). Distinct modes of floor plate induction in the chick embryo. *Development* **130**, 4809-4821.

Pons, S., Trejo, J. L., Martinez-Morales, J. R. and Marti, E. (2001). Vitronectin regulates Sonic hedgehog activity during cerebellum development through CREB phosphorylation. *Development* **128**, 1481-1492.

Rodriguez, I. and Basler, K. (1997). Control of compartmental affinity boundaries by hedgehog. *Nature* **389**, 614-618.

Roy, S. and Ingham, P. W. (2002). Hedgehogs tryst with the cell cycle. *J. Cell Sci.* **115**, 4393-4397.

Rubenstein, J. L., Martinez, S., Shimamura, K. and Puelles, L. (1994). The embryonic vertebrate forebrain: the prosomeric model. *Science* **266**, 578-580.

Sanders, T. A., Lumsden, A. and Ragsdale, C. W. (2002). Arcuate plan of chick midbrain development. *J. Neurosci.* **22**, 10742-10750.

Sasaki, H., Nishizaki, Y., Hui, C., Nakafuku, M. and Kondoh, H. (1999). Regulation of Gli2 and Gli3 activities by an amino-terminal repression domain: implication of Gli2 and Gli3 as primary mediators of Shh signaling. *Development* **126**, 3915-3924.

Scott, L. L., Mathews, P. J. and Golding, N. L. (2005). Posthearing developmental refinement of temporal processing in principal neurons of the medial superior olive. *J. Neurosci.* **25**, 7887-7895.

Stone, D. M., Hynes, M., Armanini, M., Swanson, T. A., Gu, Q., Johnson, R. L., Scott, M. P., Pennica, D., Goddard, A., Phillips, H. et al. (1996). The

tumour-suppressor gene patched encodes a candidate receptor for Sonic hedgehog. *Nature* **384**, 129-134.
Tabata, T. and Takei, Y. (2004). Morphogens, their identification and regulation. *Development* **131**, 703-712.
Thibert, C., Teillet, M. A., Lapointe, F., Mazelin, L., Le Douarin, N. M. and Mehlen, P. (2003). Inhibition of neuroepithelial patched-induced apoptosis by sonic hedgehog. *Science* **301**, 843-846.
Vaage, S. (1969). The segmentation of the primitive neural tube in chick embryos (Gallus domesticus). A morphological, histochemical and autoradiographical investigation. *Ergeb. Anat. Entwicklungsgesch.* **41**, 3-87.
Wechsler-Reya, R. J. and Scott, M. P. (1999). Control of neuronal precursor proliferation in the cerebellum by Sonic Hedgehog. *Neuron* **22**, 103-114.
Wijgerde, M., McMahon, J. A., Rule, M. and McMahon, A. P. (2002). A direct requirement for Hedgehog signaling for normal specification of all ventral progenitor domains in the presumptive mammalian spinal cord. *Genes Dev.* **16**, 2849-2864.
Yamamoto, Y. and Henderson, C. E. (1999). Patterns of programmed cell death in populations of developing spinal motoneurons in chicken, mouse, and rat. *Dev. Biol.* **214**, 60-71.
Zervas, M., Millet, S., Ahn, S. and Joyner, A. L. (2004). Cell behaviors and genetic lineages of the mesencephalon and rhombomere 1. *Neuron* **43**, 345-357.
Zervas, M., Blaess, S. and Joyner, A. L. (2005). Classical embryological studies and modern genetic analysis of midbrain and cerebellum development. *Curr. Top. Dev. Biol.* **69**, 101-138.
Zhang, X. M., Ramalho-Santos, M. and McMahon, A. P. (2001). Smoothened mutants reveal redundant roles for Shh and Ihh signaling including regulation of L/R asymmetry by the mouse node. *Cell* **105**, 781-792.